

Measurement of studded shoe-surface interaction metrics during *in situ* performance analysis

Heather Driscoll^a, John Kelley^a, Bob Kirk^b, Harald Koerger^b and Steve Haake^a

^a *Centre for Sports Engineering Research, Sheffield Hallam University, Sheffield, UK*

^b *ait. adidas-innovation-team, adidas-AG, World of Sports, 91074 Herzogenarauch, Germany*

Corresponding author: Dr Heather Driscoll, Centre for Sports Engineering Research, Sheffield Hallam University, Collegiate Crescent, Sheffield, S10 2BP UK
Phone: +44 (0) 114 225 3987 Email: H.F.Driscoll@shu.ac.uk

Acknowledgements

The authors would like to thank adidas-AG for their financial support and Professor Keith Davids, Dr Tom Allen, Dr Simon Goodwill, and Jim Emery for their constructive feedback.

References removed to maintain the integrity of the review process:

[21] Driscoll HF (2013) Understanding shoe-surface interactions. Doctoral Thesis, Sheffield Hallam University

Measurement of studded shoe-surface interaction metrics during *in situ* performance analysis

Abstract

Interaction between studded footwear and performance surfaces plays an important role in sport. Discretising this interaction into quantifiable measurements can help optimise design of outsoles and identify parameters for performance testing *in situ*. Here we describe the development and validity of an image based three-dimensional (3D) measurement system to investigate shoe-surface interactions during locomotion performance *in situ* by eight skilled footballers. By calculating individual stud positions, results revealed that the 3D kinematic data could be distilled to a number of shoe-surface interaction metrics such as orientation, velocity, translation distance and location of the centre of rotation. Findings show how the measurement system and simple analysis methods can be used to provide informative shoe-surface interaction metrics from *in situ* performance capture for the footwear community.

Keywords

Shoe-surface interactions, Studded boot, Stud configuration, Traction testing, Photogrammetry, *In situ* performance analysis

1 Introduction

Studded sports shoes are used primarily for natural turf based sports such as football (all codes), rugby and field hockey. They are perceived by many as a tool [1] forming the fundamental link between an athlete and a surface. How a shoe interacts with a surface has been shown to influence athlete performance [2] and can provide insights in estimating the likelihood of injury. In physics, the term *interaction* refers to the transfer of energy between objects; for shoe-surface interactions we are primarily concerned with a surfaces' ability to resist the motion of a shoe, i.e. the transfer of kinetic energy from a shoe to a surface. Shoe-surface interactions can be divided into two resistive components: vertical and horizontal. Vertical resistance to motion of a shoe by a surface evidences the ability of a studded outsole to penetrate the surface. Stud penetration is considered to be influenced by surface hardness and stud shape [3]. Horizontal resistance of motion between the outsole of a shoe

1 and a surface is known as traction [4], the level of which can be altered by modifying the outsole stud
2 configuration or stud profile [5] and is also dependent upon surface condition [6].
3

4
5 To quantify shoe-surface interactions mechanical tests are often used to manipulate outsoles across surfaces;
6 ranging from penetrometers to motor-driven traction test devices [5-9]. Traditionally two types of mechanical
7 tests are used to assess traction: (1) measuring the translational traction by pulling a studded shoe or plate across
8 a surface and recording the resistance to motion, or (2) determining the rotational traction by measuring the
9 torque required to rotate a shoe or plate when in contact with a surface. Mechanically quantifying a surface in
10 this way enables researchers to develop their understanding of the 'micro' level interaction between the studs and
11 a surface; for example how soil or rubber particles displace when a stud ploughs through a surface. A problem
12 arises when mechanical test results are erroneously extrapolated to infer how a human will perform with a shoe
13 and/or on a surface being tested. This is because the resulting shoe-surface interaction is not only dependent on
14 the mechanically measured properties of the shoe or surface, but also on the dynamic movement patterns of
15 individual athletes ('macro' level interaction). These movement patterns are often unique to each athlete and can
16 vary with each performance trial [10]. Individual constraints and neuromusculoskeletal strategies (for example,
17 due to prior experiences or perception on the how the outsole will perform) can all influence how an athlete
18 organises movements, whether consciously or not [11]. An outsole design based purely on mechanical test
19 measurements can often have conflicting responses when actively used by an athlete during performance. For
20 example, bladed stud configurations have been shown to have comparatively lower rotational traction measured
21 mechanically [12], but yet, are often cited (especially in the UK media) as the contributing factor to lower limb
22 injuries caused by excessive stud fixation [13]; both may be true but offer contradictory outcomes. For these
23 reasons we sought to advance understanding by analysing shoe-surface interactions when shoes are worn by
24 participants under *in situ* dynamic performance constraints to complement data from analyses when a shoe-
25 surface combination is tested mechanically.
26
27
28
29
30
31
32
33
34
35
36
37
38
39
40
41
42
43
44
45
46
47

48 If mechanical tests are to be used to infer human performance (mechanical traction testing has the advantage of
49 being more repeatable and less subjective [14]), the tests need to be representative of task performance.
50 Conducting both mechanical and human performance testing is an optimal strategy (as recommended by
51 Frederick [15] and Nigg [16]), but is not always possible, especially when time constraints dictate the level of
52 testing. This is important since replicating a complete movement (of, for example, an observed injury scenario)
53 with a mechanical device may not provide useful insights into shoe design due to significant levels of individual
54
55
56
57
58
59
60
61
62
63
64
65

1 movement pattern variability observed during actual human performance. Here we demonstrate how a shoe's
2 interaction with a playing surface can be discretised into a number of quantifiable measures during *in situ*
3 performance analysis. In essence, we observe shoe-surface interactions during performance of a complex
4 biomechanical movement and distil it down into an achievable engineering solution. Measures from such *in situ*
5 performance analyses should better inform parameters for mechanical testing allowing them to replicate task
6 performances or influence design changes for footwear.
7

8
9
10
11
12
13 Kirk *et al.* [17] first introduced the notion that kinematic information could be used to inform outsole design. A
14 single high-speed video camera was used to calculate the orientation and velocity of a shoe during realistic
15 soccer movements on a natural turf surface. However, the study was limited to two-dimensions (2D) and no
16 information was available when the studs were obscured from view (i.e. during surface penetration). To further
17 develop this methodology to include three-dimensional (3D) analysis, multiple cameras are generally required,
18 termed stereo-photogrammetry. Commercial motion capture systems are commonly used within the
19 biomechanics community to collect such data, but are often restricted to a laboratory environment, are expensive
20 and may involve intrusive marker set-ups, all of which may modify participant performance behaviours [18]. In
21 this study we describe the development of a relatively inexpensive motion capture system intended to minimise
22 potential interference with participant behaviour. An image based measurement system was also designed to
23 calculate the position of individual outsole studs during interactions with a performance surface.
24
25
26
27
28
29
30
31
32
33
34
35

36 **2 Methodology**

37
38
39 The 3D measurement system first used stereo-photogrammetry to capture the motion of participants' shoes
40 while they perform athletic movements in any test environment (for example, in a laboratory but especially
41 outside *in situ* on a natural playing field). To progress the previous work of Kirk *et al.* [17], rigid body
42 calculations were used to calculate stud locations enabling their position to be estimated even when obscured
43 from view (i.e. during surface contact). Shoe-surface interaction metrics were next identified from the
44 information on individual stud location. Although the approach of using stereo-photogrammetry to capture
45 biomechanical motion data is not novel, an important advance in this study concerns the integration of such a
46 system for calculation of stud location and corresponding shoe-surface interaction analysis whilst participants
47 performed movements. The development of the data collection system and post processing techniques are
48
49
50
51
52
53
54
55
56
57
58
59
60
61
62
63
64
65

discussed below. An adidas Copa Mundial soccer shoe was used in the following methodology sections, although the same procedure can be applied to use of any studded outsole.

2.1 Motion capture

Stereo-photogrammetry

Two high-speed video cameras (Phantom v4.3) were positioned approximately 5 m away from the test zone at an angle of 70° to each other. The following camera settings were used: 1000 fps, exposure 70 μ s, 0.6 s event duration and resolution of 512 x 382 pixels. The cameras were calibrated using the planar (checkerboard) technique [19, 20]. A maximum calibration re-projection error of ± 0.4 pixels (approximately ± 0.8 mm) was calculated for a test volume of approximately 1.5 x 1.5 x 1.0 m³. A global coordinate system was defined at the centre of the test volume such that the y axis was in the direction of motion, the x axis was medial to the direction of motion and the z axis was vertical.

Marker tracking algorithm

Four, white high contrast markers (retro-reflective paint, 8 mm diameter) were positioned on the left shoe and were used to define two rigid bodies representing the rear-foot and forefoot sections of a shoe (Fig. 1a). A semi-automated tracking method was developed using MATLAB[®] image processing algorithms to allow fast and efficient acquisition of marker coordinates. The tracking tool required the user to first select the marker and input the number of frames over which to track. Self-windowing and binary conversions were then used to automatically identify the selected marker over the remaining frames, returning the 2D image coordinates of the marker. If no marker was found, a predicted position was calculated from the marker positions at the previous two time-steps, until the marker could be detected again. Stereo-triangulation was used to convert the 2D image coordinates from the left and right camera views into 3D global coordinates. The 3D coordinates were smoothed using a five-point moving average filter.

2.2 Calculation of stud position

1 The assumption was made that the shoe acted as two rigid bodies rotating about a hinge axis running
2 approximately medial-laterally and positioned near the metatarsal-phalangeal joint. The rear-foot rigid body was
3 defined by three markers positioned on the lateral side of the shoe near the heel (P1), ankle (P2) and proximal to
4 the metatarsal-phalangeal joint (P3). The forefoot rigid body was defined by a fourth marker at the toe (P4) and
5 two pseudo-markers (P5 and P6) positioned on the lateral and medial sides of the hinge axis (Fig. 1a). Fixed
6 position markers were not used for the forefoot section as excessive deformation of a shoe upper rendered it
7 difficult to position a marker without invalidating the rigid body assumption. The shoe consisted of 12 studs,
8 four on the heel and eight on the forefoot; the heel studs and the rear most stud on the lateral side of the forefoot
9 were associated with the rear-foot rigid body, and the remaining studs with the forefoot rigid body (Fig. 1b). The
10 rear-foot and forefoot stud allocation was based on observation of the shoe flexing about the forefoot during a
11 heel-strike to push-off walking movement.
12
13
14
15
16
17
18
19
20
21
22

23 Fig. 1a and 1b about here
24
25

26 The following protocol was used to calculate the stud positions during movement trials:
27
28

- 29 (1) The stud and marker coordinates of the shoe were measured in a static reference position;
- 30 (2) The hinge axis position and direction was calculated from a heel-plant to toe-off walking trial;
- 31 (3) Two pseudo-markers on the medial and lateral sides of the shoe on the hinge axis were calculated;
- 32 (4) The pseudo-marker locations were defined relative to the static reference position;
- 33 (5) Transformation matrices from side marker to stud position for the rear-foot and forefoot using the
34 reference position were calculated;
- 35 (6) The side markers were tracked during a movement trial using the semi-automated tracking algorithm;
- 36 (7) Inverse transformations were applied to obtain the stud positions.
37
38
39
40
41
42
43
44
45
46
47

48 *Reference position of studs and markers* 49 50

51 A shoe was placed on a flat glass surface and positioned such that the rear most heel studs (S1, lateral side and
52 S2, medial side) and rear most forefoot stud (S3, lateral side) formed a local coordinate system (where S1 =
53 origin, S1 to S2 = x axis and S1 to S3 = y axis). Shoe markers were measured relative to the local coordinate
54 system using a right-angled arrangement of metal rulers (accuracy ± 0.5 mm) perpendicular and parallel to the
55 axis system. The glass surface and shoe were then rotated such that the studs were visible. The centre of the
56
57
58
59
60
61
62
63
64
65

1 studs (x, y position) were then measured relative to the local coordinate system (accuracy ± 0.5 mm), with the
2 vertical (z) coordinate measured using digital callipers (distance from the centre of the stud to the glass plate
3 surface, accuracy ± 0.1 mm). The position of each stud and marker in the local coordinate system were recorded
4 and saved as the reference position.
5
6

7 8 9 *Identifying a hinge axis*

10
11 To identify the hinge axis between the rear-foot and forefoot rigid bodies a participant was asked to walk
12 through the stereo-calibrated volume performing a heel-plant to forefoot push-off. One trial of this movement
13 was required for each participant from the data collection study cohort. This allowed the hinge axis position to
14 be customised to the individual, increasing the validity of the two rigid-bodies assumption. The three rear-foot
15 markers were tracked during the movement and data were obtained on the position and direction of the hinge
16 axis (Fig. 2) using the following methodology:
17
18
19
20
21
22
23
24

- 25 (1) A time period (t_1 to t_2) in which the forefoot studs of the shoe were observed to be fully in contact with
26 the surface and rear-foot studs were out of contact was identified from the video footage.
27
- 28 (2) The position vectors of the rear-foot markers were identified at the start and end of the selected time
29 period (P1, P2, P3 at t_1 and P1', P2', P3' at t_2).
30
- 31 (3) Three planes were calculated: one plane defined as equidistant from P1 and P1', another equidistant
32 from P2 and P2' and the final plane equidistant from P3 and P3'.
33
34
- 35 (4) Any pair of these three planes could be used; however, the two planes with the greatest angle between
36 were selected to reduce relative effect of errors.
37
38
- 39 (5) The line of intersection between the two selected planes was calculated to give the rotation or hinge
40 axis.
41
42
43
44
45
46

47 Fig. 2 about here
48
49
50

51 *Pseudo-marker location*

52
53 The above methodology defined the location of the hinge axis in the global coordinate system during the
54 selected walking trial. The next stage was to use the hinge axis to define two pseudo-markers that could be used
55 to complete the rigid body of the forefoot section. First, a plane containing the three rear-foot markers (P1, P2
56
57
58
59
60
61
62
63
64
65

1 and P3) at the first time step was calculated. The point of intersection of this plane and the line through the
2 rotation axis was then determined; this formed the first pseudo-marker (P5) (Fig. 2). A second point 100 mm
3 along the hinge axis from P5 was calculated to determine the second pseudo-marker (P6). A distance of 100 mm
4 was selected for the second pseudo-marker; this distance is arbitrary, but in this instance it approximately related
5 to the width of the forefoot. In order for the pseudo-markers to be used in other trials, their position relative to
6 the marker P4 needed to be defined. This required calculating a transformation matrix to determine the pseudo-
7 marker position in the reference frame. The process of obtaining the transformation matrix formed an integral
8 part of the methodology and is used a number of times to obtain the final stud position.
9
10
11
12
13
14
15
16
17

18 *Transformation matrix*

19 The transformation matrix, [M] was calculated in MATLAB[®] and defined as follows:
20
21
22

$$23 \quad [M] = [R][T] \quad (1)$$

24 where [T] is the translation matrix to set P1 to the origin and [R] is the rotation matrix for an XZY rotation
25 sequence in which P3 is firstly rotated onto the x-y plane, then onto the y-z plane and finally P2 is rotated onto
26 the x-y plane.
27
28
29
30
31
32
33

34 Equation 1 was used to calculate the transformed position of the rear-foot studs when using P1, P2 and P3. The
35 transformed position of the pseudo-markers and P4 were then calculated relative to P1, P2 and P3. Finally, the
36 forefoot studs were transformed relative to P5, P6 and P4 (replacing P1, P2, P3 respectively in the above
37 calculation).
38
39
40
41
42
43
44

45 *Calculating final stud position*

46 To obtain the final stud positions during each movement trial firstly required the side markers to be tracked and
47 converted to 3D coordinates. The rear-foot marker coordinates were then transformed using Equation 1 and the
48 inverse transformation matrix, [M]⁻¹ used to obtain the rear-foot stud positions and the pseudo-marker positions.
49 The pseudo-markers and forefoot marker were then transformed as above and the inverse transformation matrix
50 used to determine the forefoot stud locations. Knowledge of stud location during each movement trial yielded
51 further information such as time of surface contact of individual studs.
52
53
54
55
56
57
58
59
60
61
62
63
64
65

2.3 Calculation of shoe-surface interaction metrics

Orientation

The orientation of the shoe was defined using the local coordinate system on the rear-foot of the shoe. The three Euler angles (pitch, yaw and roll) were calculated using the direction cosine matrix formed by transforming the local coordinate system onto the global coordinate system. The MATLAB[®] script used to calculate the transformation matrix was again used, substituting the side markers (P1, P2 and P3) for the three stud positions (S1, S2 and S3 respectively). The pitch angle corresponded to the first rotation about the x-axis, the yaw angle the second rotation about the z-axis and finally, the roll angle was the last rotation about the y-axis. The pitch, yaw and roll angles were non-commutative and are reported in degrees. Positive pitch angles corresponded to the shoe being in a toe-up position, positive yaw to a toe-in position and positive roll corresponded to an outward rotation of the shoe.

Velocity and acceleration

The velocity of each stud was derived from stud coordinates using the central differencing method over five time steps and smoothed using a five-point moving average filter [21]. Acceleration was calculated from the unfiltered velocity data using a three-point central differencing method.

Translation

Translation of the shoe (or slip) was defined as being a period of significant stud motion in the horizontal direction with little or no motion in the vertical direction, and/or with little or no change in pitch angle during stud-surface contact. These constraints eliminated the likelihood that the change in horizontal motion was due to the shoe lifting off the surface. The stud coordinates during surface contact were also viewed on a 2D horizontal plane (turf surface) to note the dominant motion direction during the movement; the plots produced using this approach were known as the stud translation vectors.

Rotation

1 The 2D centre of rotation of the shoe during contact with the surface was calculated using the Reuleaux method.
2 The Reuleaux method states that the displacement of any rigid body in 2D can be represented by a rotation of
3 angle, θ about a pole of displacement (or centre of rotation, I), if the location of two points on the rigid body are
4 known (stud positions) (Fig. 3). Full details of the Reuleaux method can be found in the paper by Eberharther and
5 Ravani [22].
6
7
8
9

10 **3 Validation and error analysis**

11 **3.1 Stereo-photogrammetry and marker tracking**

12 *Reliability*

13
14
15 The reliability of the semi-automated tracking algorithm was assessed by tracking two markers over 26 frames
16 and repeating five times for both the left and right camera images. The standard deviation of the distance
17 between image coordinates of the markers from the five repeats was averaged to give the mean standard
18 deviation in pixels. The mean standard deviation in marker coordinates tracked using the semi-automated
19 algorithm was ± 0.25 pixels. Propagating this to 3D global coordinates after stereo-triangulation led to a mean
20 standard deviation of ± 0.5 mm.
21
22
23
24
25
26
27
28
29
30
31
32
33

34 *Repeatability*

35
36
37 To assess the error arising from changes in test conditions, camera position and participant repeatability, a
38 reliability study was carried out over two separate test days. The same participant was involved in both tests and
39 was asked to perform a sprint movement five times. The same cameras were used for testing but the position
40 varied between the two test days. The velocity of marker P3 in the vertical direction at touch-down was used for
41 comparison. The mean velocity from the five trials on each test day was calculated. The absolute difference
42 between the two mean velocity values was 0.18 ms^{-1} . A *t*-test indicated that there was no significant difference
43 between the impact velocities at the $p = .10$ level. It is likely that differences observed were due to participant
44 familiarity rather than the measurement system, indicating that in future research a habituation period prior to
45 testing may be required.
46
47
48
49
50
51
52
53
54
55
56
57
58
59
60
61
62
63
64
65

Validation

The 3D marker coordinates resulting from the stereo-photogrammetry method and tracking algorithm were validated by comparison with a laboratory based Motion Analysis Capture (MAC) system. The MAC system is reported to have an accuracy of 0.1 mm [23] and was considered the gold standard for this analysis. A reflective marker was rotated in a circular horizontal trajectory at a constant rotational velocity of 60.0 rpm and fixed radius of 400 mm using a motor driven device. A second static marker was placed on the rotation centre of the device. Both markers were tracked using eight infrared cameras for the MAC system and two high-speed cameras for the stereo-photogrammetry method. The coordinates obtained from the MAC system were compared to the results from the stereo-photogrammetry system after stereo-triangulation. The radius of rotation was calculated from the resultant distance between the static marker and the rotating marker. A mean over 147 time-steps (0.588 s) was calculated and compared to the true value of 400 mm. The mean angular velocity was further calculated from the angular displacement of the rotating marker relative to the static marker and compared to the true value, 60.0 rpm (6.28 rad/s). Both tracking systems were within 99% of the true values for both the radius and angular velocity (Table 1), suggesting that the stereo-photogrammetry system was acceptable for use in motion capture scenarios.

Table 1 about here

3.2 Stud position and contact timing

To verify the time of initial stud-surface contact (touch-down), the stereo-photogrammetry system was synchronised with a force plate (Kistler 9281) sampling at 1000 Hz. A falling edge trigger with a 5 N threshold was used to define the time of touch-down from the force data. The time of peak vertical acceleration of marker P3 was used to define touch-down from the kinematic stereo-photogrammetry data. The agreement between the two events suggested that it was appropriate to use the peak acceleration of marker P3 to define touch-down when force data were unavailable (for example, in ecological test environments). A similar approach was used by Hreljac and Marshall [24] in determining event timing with kinematic data during walking.

Individual stud contact timings and positions were evaluated by comparison to the results obtained from performing the test on a pressure-mat (RSscan footscan®, 2D plate 0.5 m, 200 Hz). A participant was asked to walk across the pressure-mat performing a heel-plant to toe push-off movement. The pressure results

1 from the mat enabled the time of contact to be determined. The initial contact time of each stud was obtained
2 and compared to the predicted contact time from the stereo-photogrammetry system (Fig. 4). As it was not
3 possible to synchronise the two measurement systems, the first stud to contact the surface (S1) was set to time 0
4
5
6 s.

7
8
9 Fig. 4 about here

10
11
12 The mean absolute difference between stud contact detected by the pressure mat and that estimated from stereo-
13 photogrammetry was 0.033 ± 0.031 s. The closest match was seen for the heel studs (S1, S2, S4 and S5), with a
14 mean absolute difference of 0.016 s, the stereo-photogrammetry system indicated a slight delay in detecting
15 contact for the heel studs. The mid-foot studs (S3, S6, S7 and S8) were also in good agreement, with a mean
16 absolute difference of 0.033 s. The toe studs (S9, S10, S11 and S12) showed the greatest difference with a mean
17 absolute difference of 0.051 s, in general the stereo-photogrammetry system predicted contact earlier for the toe
18 studs than that seen by the pressure mat. The mid-foot and toe studs were calculated from the forefoot rigid
19 body using the pseudo-markers on the hinge-axis. It was anticipated that this additional calculation would
20 increase the error in stud location prediction, but comparison with the pressure mat data revealed that the
21 differences seen in contact time between studs were not significant (Spearman's rho $\rho = .96$).
22
23
24
25
26
27
28
29
30
31
32

33 **4 Practical assessment**

34 4.1 Pilot data collection study

35
36
37
38 To assess the feasibility of the system for collecting data and interpreting the results, a pilot data collection study
39 was carried out by observing movement performance of eight participants (following informed consent and
40 approval from the institution's ethics committee) from Doncaster Rovers Youth Development Team (17.1 ± 0.5
41 years). Participants were asked to complete five repetitions of an acceleration movement (6 m jog followed by 6
42 m sprint) selected as it required high levels of traction and was similar to that used by Kirk *et al.* [17]. Data
43 collection took place on a natural grass surface (FIFA standard ball rebound of 40%). The stereo-
44 photogrammetry technique and tracking algorithm were used to track the shoe markers for each trial. A time
45 period in which the forefoot of the shoe remained in contact with the ground and the rear-foot section rotated off
46 the surface was used to determine the hinge-axis and pseudo-marker location for each participant. Data from a
47 representative trial will be presented here to demonstrate the role of inexpensive and simple methodology and
48
49
50
51
52
53
54
55
56
57
58
59
60
61
62
63
64
65

1 analysis technique for sampling shoe-surface interaction information from *in situ* movement performance. The
2 use of single trial analysis has been previously justified in the literature [10] and is relevant due to the inherent
3 variability present in human kinematic behaviour in line with the premise that "averaging" performance data
4 across participants can often create a set of results that does not resemble any of the individual trials.
5
6
7
8
9

10 4.2 Orientation and velocity

11
12 During the exemplar trial the shoe was observed to impact the surface in a toe-down position with the forefoot
13 studs coming into contact first at a pitch angle of -16° and impact velocity in the y-z plane of 1.5 ms^{-1} . The yaw
14 angle was -25° , such that the forefoot of the shoe rotated outwards while the roll angle was small enough to be
15 negligible (Fig. 5).
16
17
18
19
20
21

22 Fig. 5 about here
23
24
25

26 4.3 Stud contact timing

27
28 Five of the forefoot studs were observed to come into contact with the surface almost simultaneously upon foot-
29 strike. By approximately 35% stance time all the forefoot studs were in contact, throughout the movement, the
30 heel studs did not come into contact with the surface. During the push-off phase, stud S12 was the last stud to
31 remain in contact with the surface, Fig. 6 illustrates the order in which the studs left the surface.
32
33
34
35
36
37

38 Fig. 6 about here
39
40
41

42 4.4 Centre of rotation

43
44 During the midstance phase (20 - 60% stance time) of the exemplar trial, the shoe was observed to rotate
45 outwardly with greater displacement of the lateral forefoot studs compared to the medial side. The calculated
46 centre of rotation was position just outside the medial edge of the forefoot as shown in Fig. 7.
47
48
49
50
51
52

53 Fig. 7 about here
54
55

56 5 Limitations

57
58
59 The following limitations of the measurement system have been acknowledged:
60
61
62
63
64
65

- 1
2
3
4
5
6
7
8
9
10
11
12
13
14
15
16
17
18
19
20
21
22
23
24
- (1) The shoe was assumed to be comprised of two rigid bodies pivoting about a hinge axis. Calculation of the hinge axis from movement trial data allowed two pseudo-markers to be defined to form the forefoot rigid body. Deformation to either the rear-foot or forefoot rigid bodies introduces inaccuracies in the matrix transformation to calculated stud position. For future testing, further analysis into the optimum marker set and number of rigid bodies required to reduce the measurement error is recommended.
 - (2) Circular tracking markers were used which have the potential to introduce eccentricity errors; they were however less obtrusive and less prone to movement error than spherical markers. The marker size was approximately 1-2% of the total image size and as such it was expected that the error from eccentricity would be negligible.
 - (3) The calculation of the 2D centre of rotation assumed no movement occurred in the vertical axis. A 3D approach such as the helical screw axis could be used for situations where substantial motion in more than two planes occurs.

25 **6 Conclusion**

26
27
28 A method for obtaining 3D kinematic information of a studded shoe prior, during and after contact with a turf
29 surface has been established for *in situ* testing. The technique is relatively inexpensive compared to existing
30 methods and requires only two cameras with a simple calibration procedure. The markers on the shoe are
31 passive and non-obtrusive and are not likely to influence participant performance. This relatively inexpensive
32 and simple to use system has an accuracy level comparable to that of a more expensive, commercially available
33 multi-camera system (Table 1) with the considerable advantage that it can be used to analyse stud-surface
34 interactions during movement performance *in situ*. Image processing techniques allowed the footage to be
35 analysed efficiently and accurately (± 0.5 mm) with minimal user intervention. Rigid body calculations were
36 used to determine the location of the studs from the 3D position of the tracking markers. This allowed the stud
37 position to be estimated when they are occluded (for example, during penetration with the surface). Stud
38 positions were verified by comparison with performance on a pressure mat (Spearman's rho $\rho = 0.96$). The 3D
39 kinematic data were then distilled down to a number of quantifiable measures such as shoe orientation, velocity
40 or the location of the centre of rotation. More extensive data collection needs to be undertaken in future research
41 to investigate the changes in shoe movement parameters during a variety of different motions, outsole designs
42 and surfaces.
43
44
45
46
47
48
49
50
51
52
53
54
55
56
57
58
59
60
61
62
63
64
65

References

1. Torell, V.B., 2011. As fast as possible rather than well protected: experiences of football clothes. *Journal of Cultural Research*, 3, pp.83-99.
2. Müller C, Sterzing T, Lange J, Milani, T (2010) Comprehensive evaluation of player-surface interaction on artificial soccer turf. *Sports Biomech* 9(3):193-205
3. Clarke JD, Carré MJ (2010) Improving the performance of soccer boots on artificial and natural soccer surfaces. In: Sabo A, Litzenberger, S, Kafka P, Sabo C (eds) 8th Conference of the International Sports Engineering Association, 11-14 July 2010 Vienna, Elsevier Ltd., London, pp 2775-2781
4. McNitt A (2000) Traction on turf. *Grounds Maintenance* 35(9):4-9
5. Haake SJ, Carré MJ, Kirk RF, Senior T (2004) Traction of studded boots on turf. In: Hubbard M, Mehta RD, Pallis JM (eds) *The engineering of sport 5*. ISEA, pp 544-551
6. McNitt AS, Middour RO, Waddington DV (1997) Development and evaluation of a method to measure traction on turfgrass surfaces. *J Test Eval* 25(1):99-107
7. Twomey DM, Connell M, Petrass L, Otago L (2013) The effect of stud configuration on rotational traction using the studded boot apparatus. *Sports Eng* 16(1):21-27
8. Kuhlman S, Sabick M, Pfeiffer R, Cooper B, Forhan J (2009) Effect of loading condition on the traction coefficient between shoes and artificial turf surfaces. *Proceedings of Proceedings of the Institution of Mechanical Engineers, Part P: J Sports Eng Tech* 223:155-165
9. Orchard J (2001) The AFL Penetrometer Study: Work in Progress. *J Sci Med Sport* 4(2):220-232
10. Bates BT (1996) Single-subject methodology: an alternative approach. *Med Sci Sport Exer* 28(5):631-638
11. Lees A, Bouracier J (1994) The longitudinal variability of ground reaction forces in experienced and inexperienced runners. *Ergonomics* 37(1):197-206
12. Galbusera F, Tornese D, Anasetti F, Bersini S, Volpi P, La Barbera L, Villa T (2013) Does soccer cleat design influence the rotational interaction with the playing surface. *Sports Biomech*. doi:10.1080/14763141.2013.769277
13. Taylor L (2010) Steve Bruce demands inquiry into modern boots as cause of injury spate. *The Guardian*. <http://www.guardian.co.uk/football/2010/sep/16/steve-bruce-boots-injurys>. Accessed 31 October 2011
14. Clarke J, Carré M, Damm L, Dixon S (2013) The development of an apparatus to understand the traction developed at the shoe-surface interface in tennis. *Proceedings of Proceedings of the Institution of Mechanical Engineers, Part P: J Sports Eng Tech*. doi: 10.1177/1754337112469500
15. Frederick EC (1986) Kinematically mediated effects of sport shoe design: A review. *J Sport Sci* 4(3):169-184
16. Nigg BM (1990) The validity and relevance of tests used for the assessment of sports surfaces. *Med Sci Sport Exer* 22(1):131-139
17. Kirk RF, Nobel ISG, Mitchell T, Rolf C, Haake SJ, Carré MJ (2010) High-speed observations of football-boot-surface interactions of players in their natural environment. *Sports Eng* 10:129-144
18. Heller B, Haake S (2006) Pacing lights - a new approach to controlling speed in the gait laboratory. In: Mortiz EF, Haake SJ (eds) *The Engineering of Sport Vol 2: Developments for Disciplines*. Springer, New York, pp 186-201

19. Bouguet JY (2010) Camera Calibration Toolbox for Matlab. http://www.vision.caltech.edu/bouguetj/calib_doc/. Accessed 28 October 2011
20. Zhang Z (1999) Flexible camera calibration by viewing a plane from unknown orientations. Proceedings of the 7th IEEE International Conference on Computer Vision, 20-27 September 1999 Corfu, Greece: IEEE, pp 666-673
21. *Reference removed to maintain the integrity of the review process.*
22. Eberharter JK, Ravani B (2006) Kinematic registration in 3D using the 2D Reuleaux method. J Mech Design 128:349-355
23. Baroon J, Ravani B (2006) A three-dimensional generalization of Reuleaux's method based on line geometry. Proceedings of IDETC/CIE 2006, 10-13 September 2006 Philadelphia, ASME: Pennsylvania, pp 1-8
24. Richards JG (1999) The measurement of human motion: A comparison of commercially available systems. Hum Movement Sci 18:589-602
25. Hreljac A, Marshall RN (2000) Algorithms to determine event timing during normal walking using kinematic data. J Biomech 33:783-786

Tables

Table 1 Radius and angular velocity of marker trajectory (mean \pm S.D.)

	MAC	Stereo-photogrammetry	True value
Radius (mm)	398.5 \pm 0.3	399.4 \pm 0.8	400.0
Angular velocity (rad/s)	6.27 \pm 0.45	6.26 \pm 0.56	6.28

Figure captions

Fig. 1a Marker positions on the left shoe forming two rigid bodies (rear-foot and forefoot) - the dashed line indicates the pseudo-marker P6 is on the medial side of the shoe; **1b** Stud location numbering convention (studs S1, S2 and S3 form the local coordinate system) - black studs lie on the rear-foot, grey studs on the forefoot.

Fig. 2 The hinge axis was formed from the intersection of the two planes equidistant from P3-P3' and P1-P1'. The pseudo-marker is formed from the intersection of the plane through the points P1, P2 and P3 and the hinge axis. Please see Fig. 1 for the location of markers P1, P2 and P3 on the shoe.

Fig. 3a Reuleaux method used to calculate the centre of rotation from two stud coordinates (Modified from [23]) **3b** Example of shoe rotating from position P to P'

Fig. 4 Time of contact of each stud found from the pressure mat and calculated using the stereo-photogrammetry method

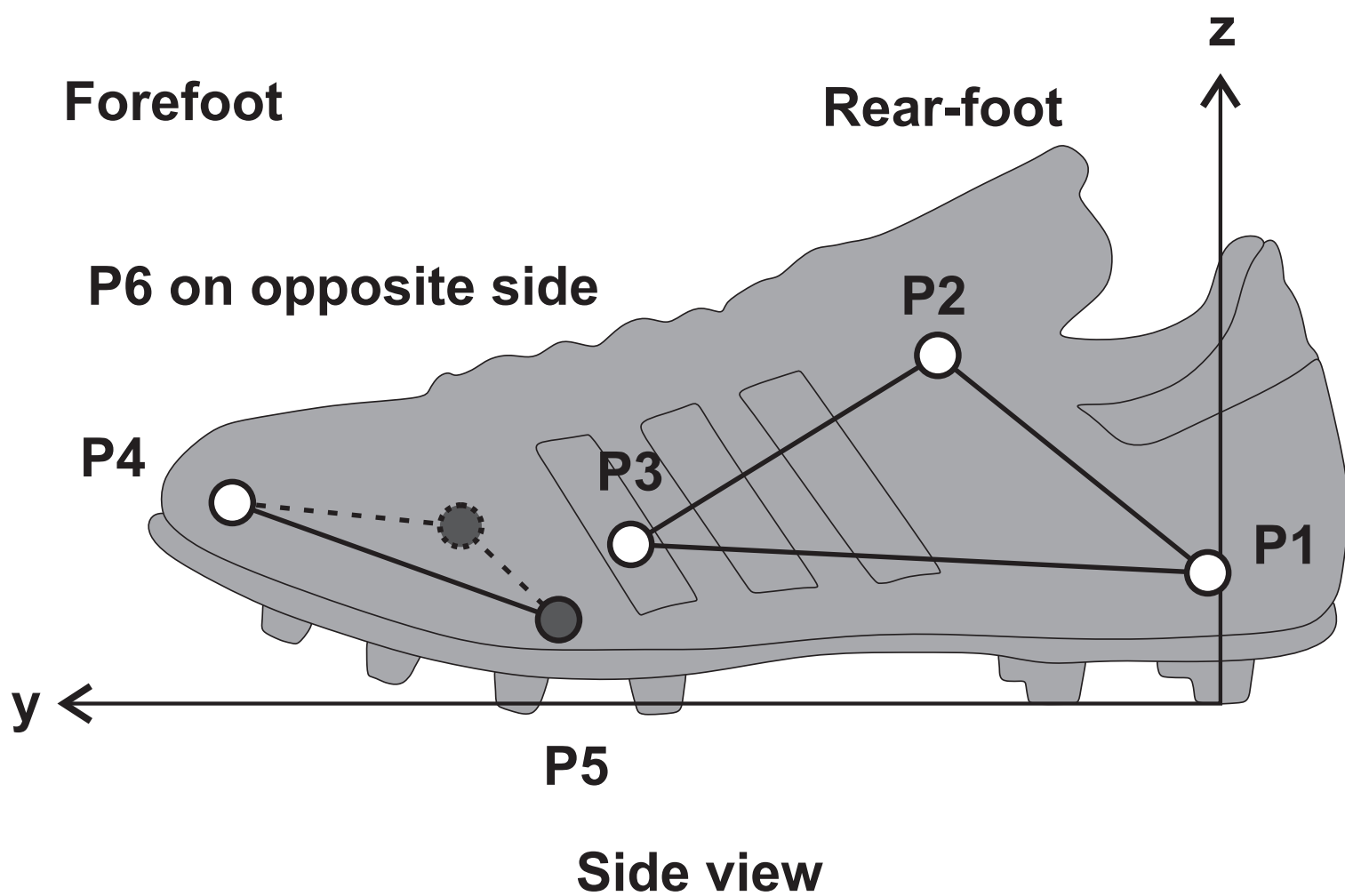
Fig. 5 Orientation and velocity vectors for the forefoot studs at touch-down for the sprint movement

Fig. 6 Time of stud release from the surface for the sprint movement (at push-off)

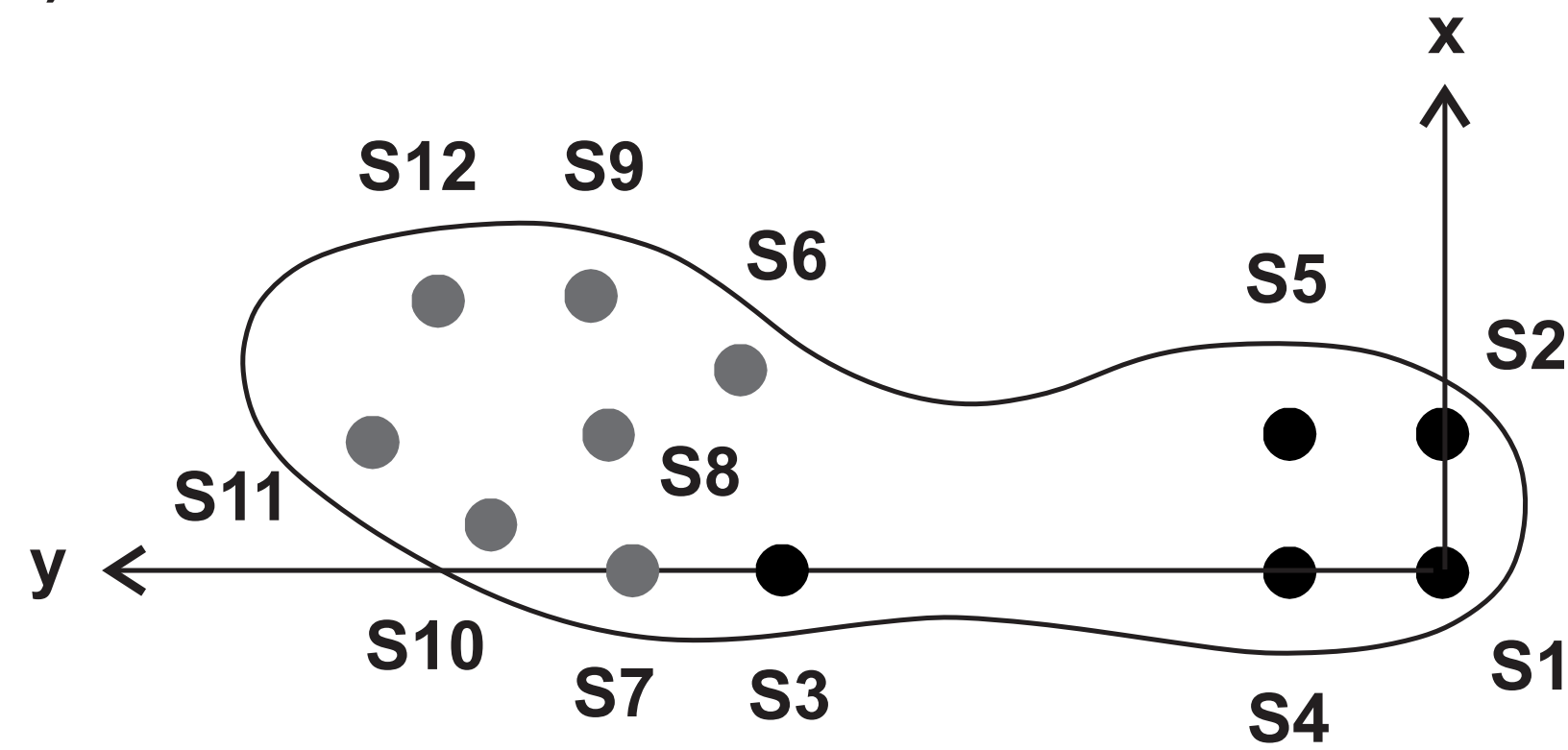
Fig. 7 Stud position and calculated centre of rotation (shaded circle represents ± 1 S.D., arrow indicates rotation direction)

Fig 1a

a)



b)



Plan view

Fig. 2

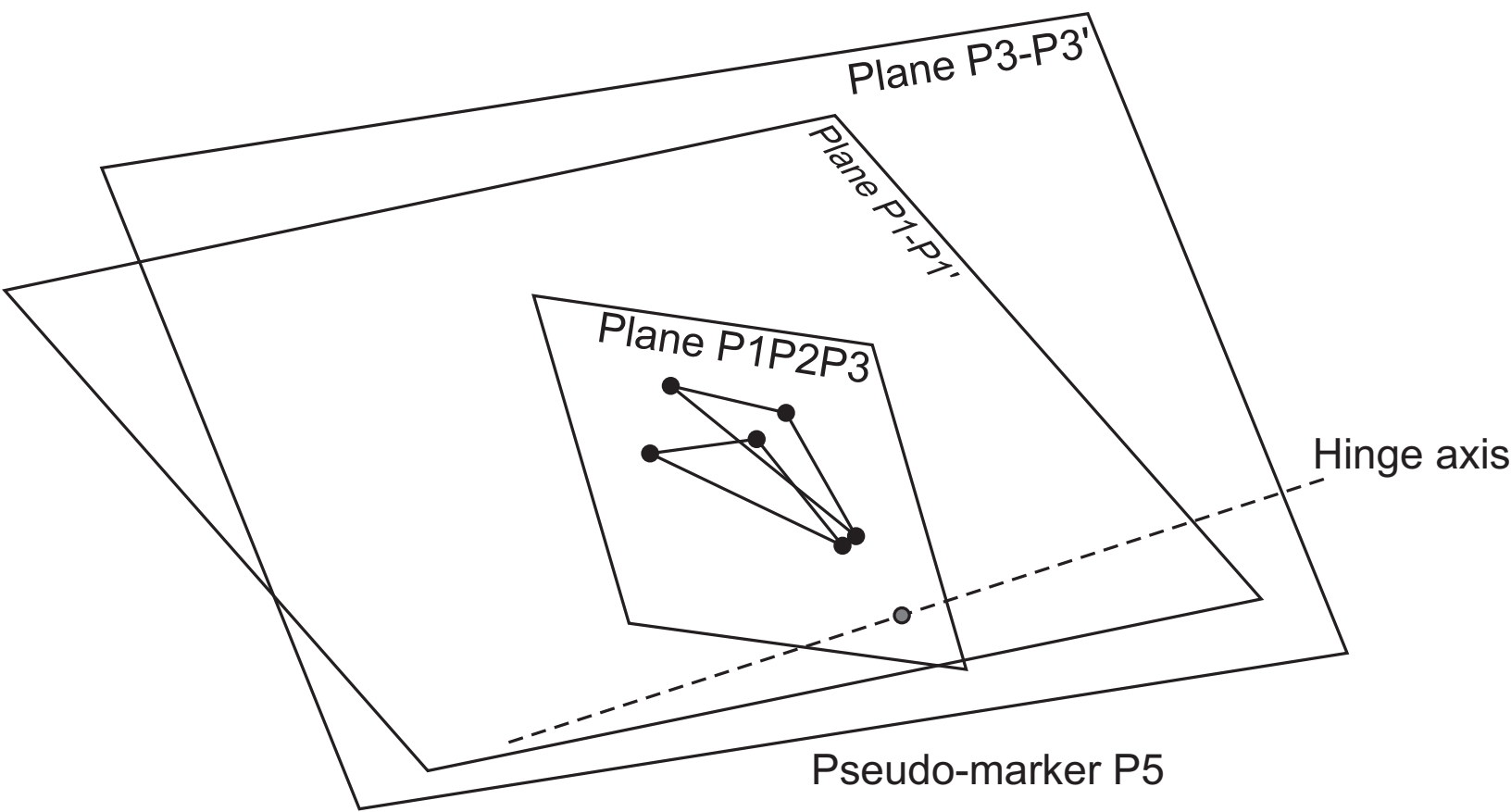
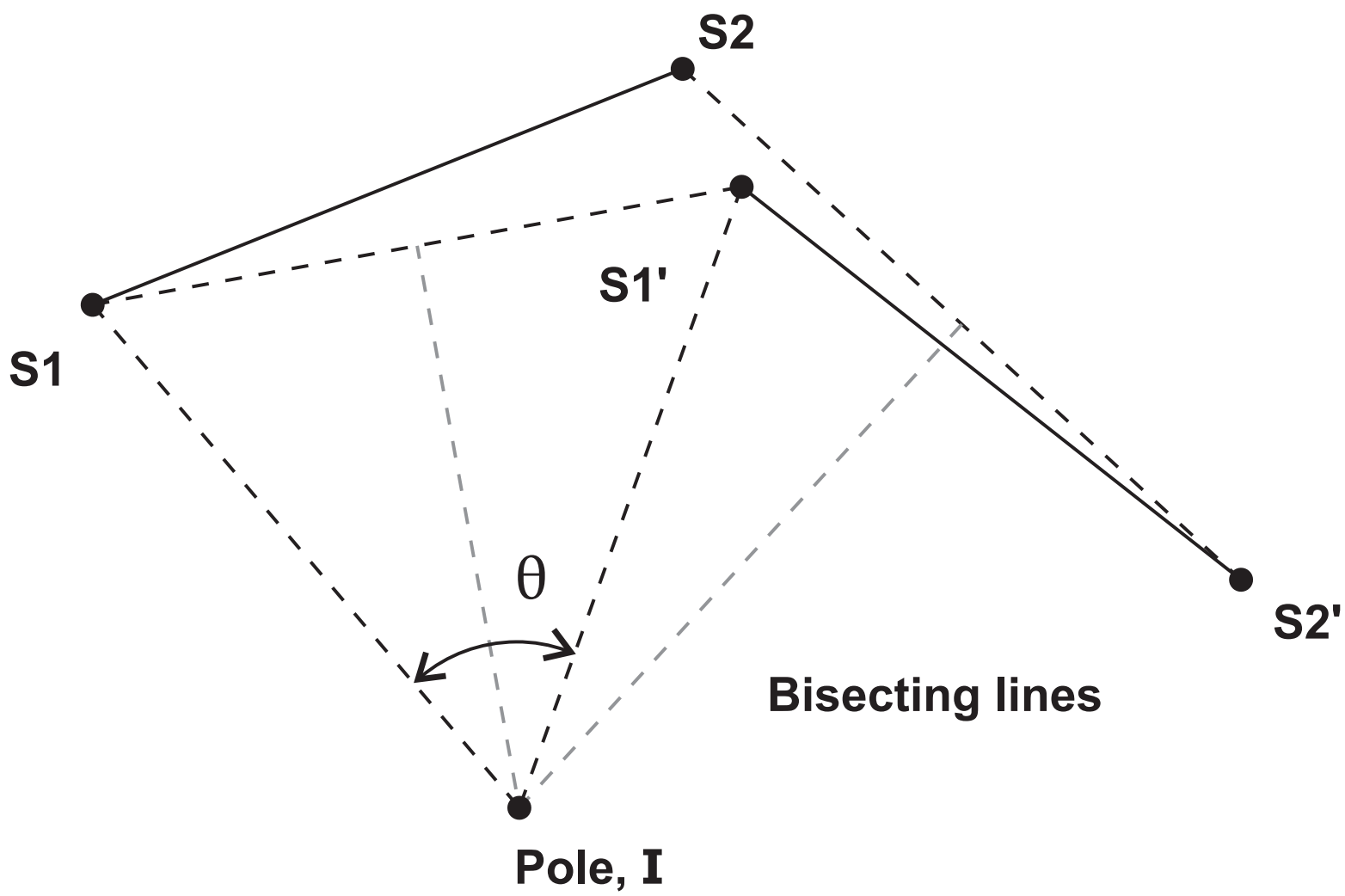


Fig 3a

a)



b)

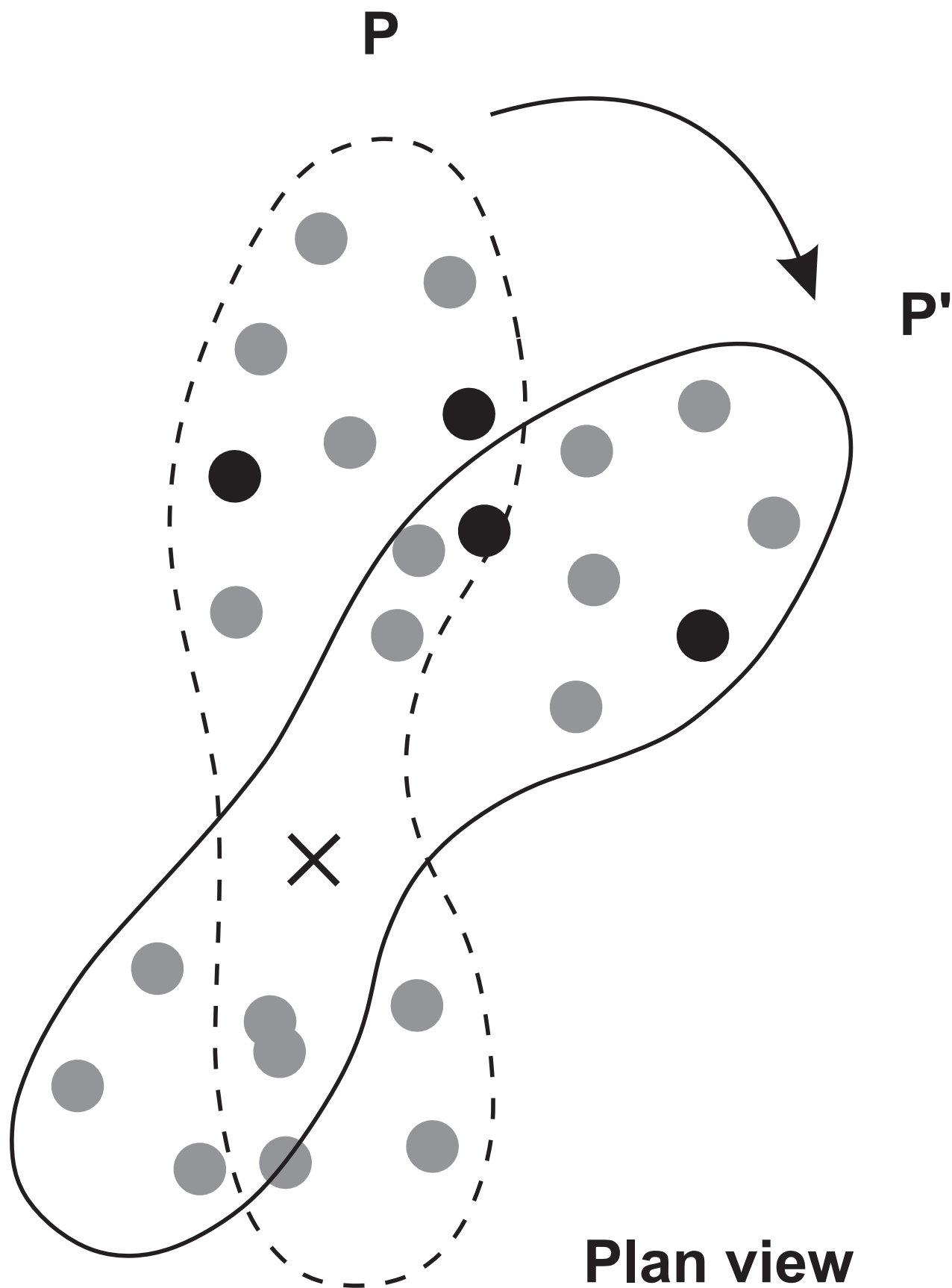


Fig. 4

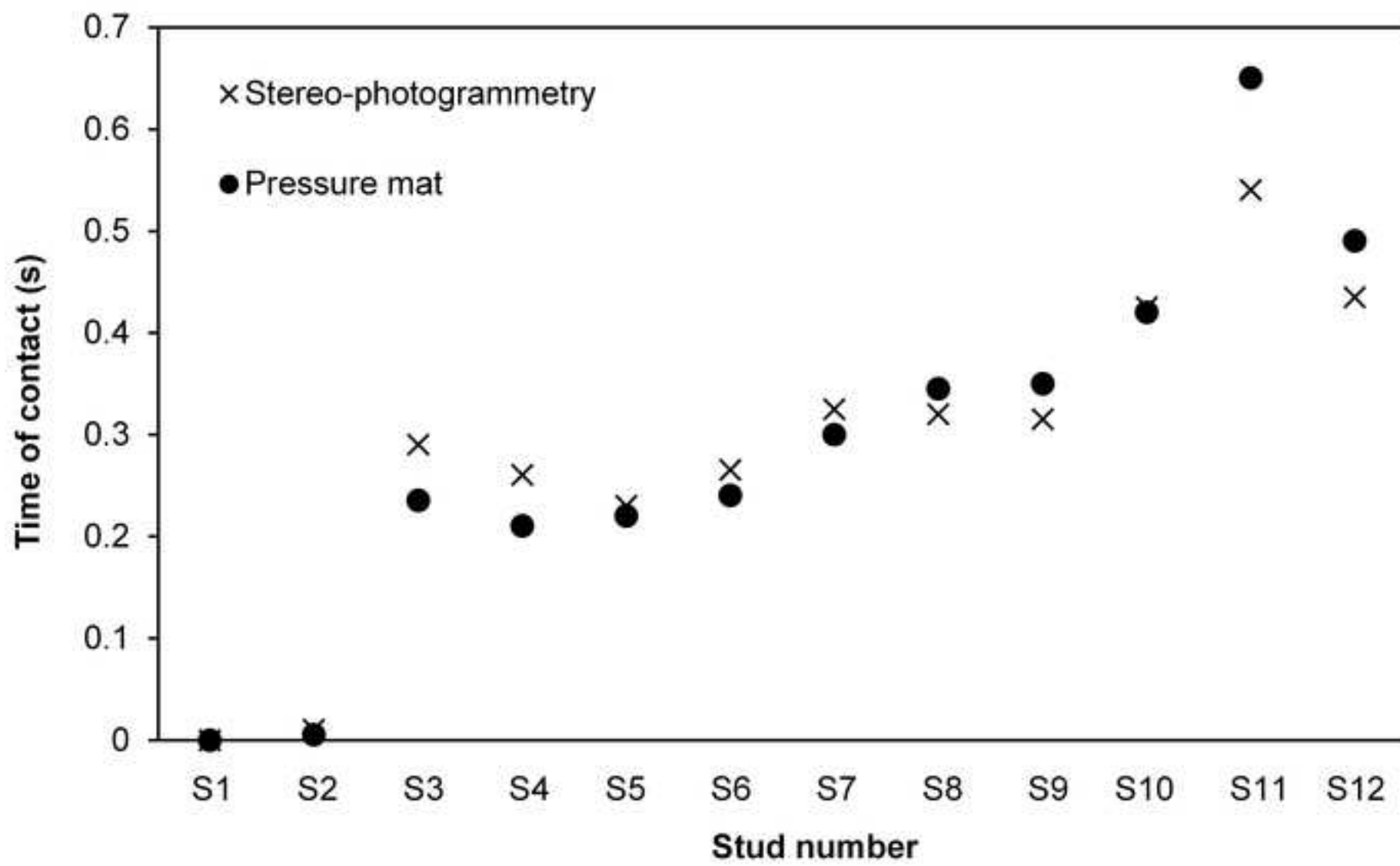
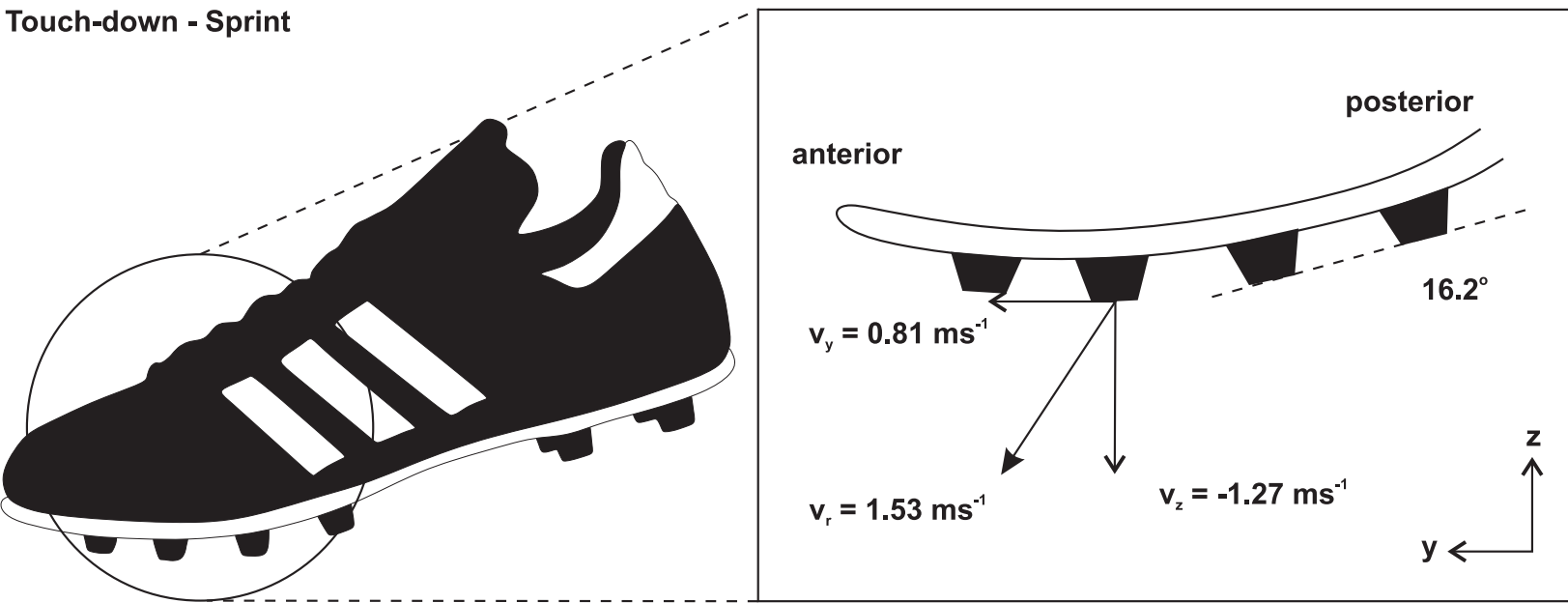


Fig 5

Touch-down - Sprint



Pitch = -16° , Yaw = -25° , Roll = -1°

Fig 6

Sprint - push-off

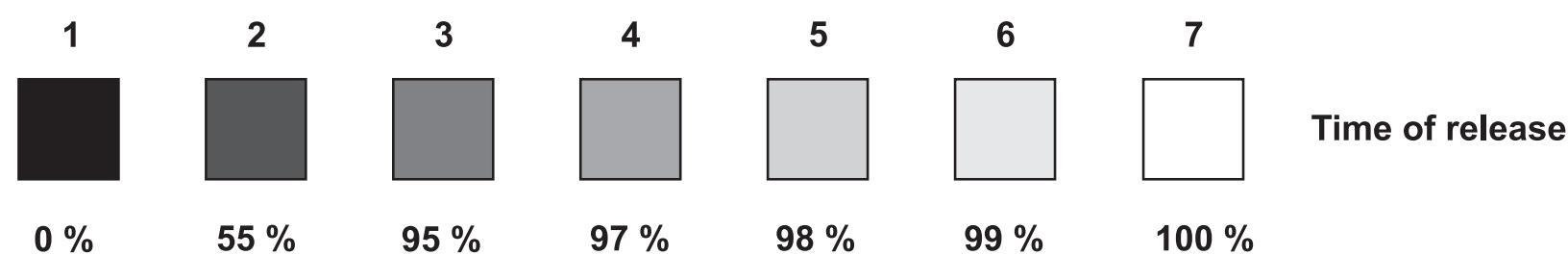
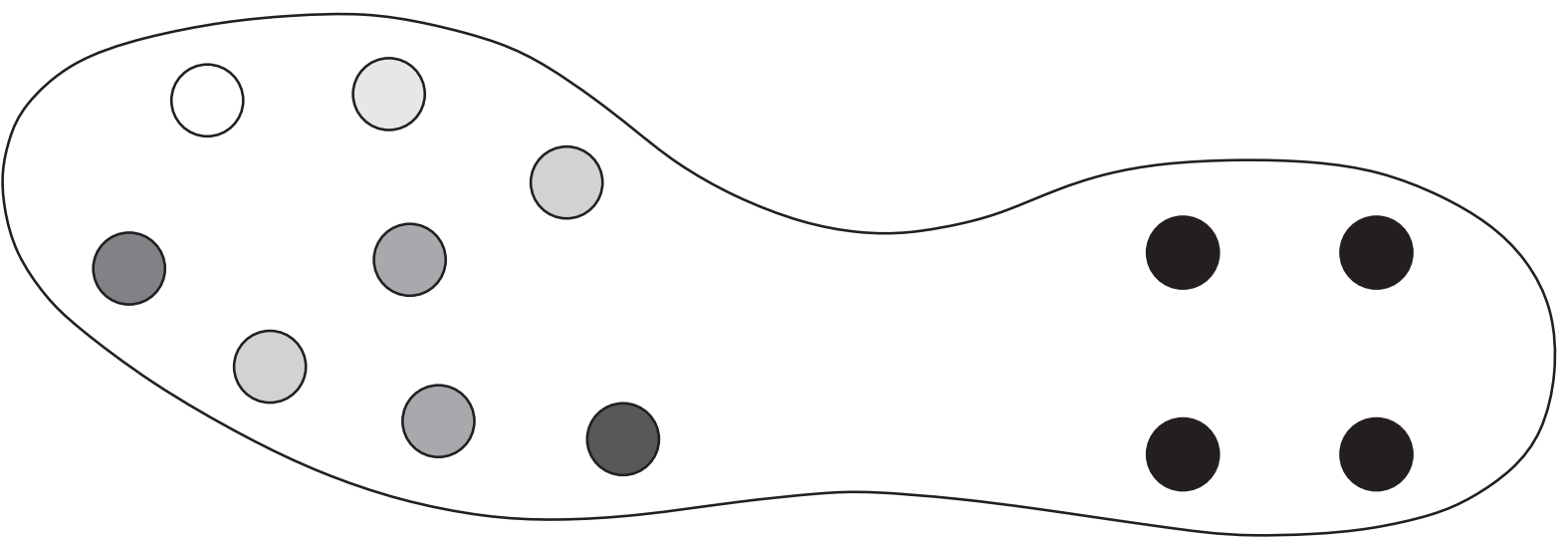


Fig. 7

